A&A 549, A133 (2013)
DOI: 10.1051/0004-6361/201219851

Astronomy & Astrophysics

VLA/JVLA monitoring of bright northern radio sources⋆

N. Kurinsky[1], A. Sajina[1], B. Partridge[2], S. Myers[3], X. Chen[4], and M. López-Caniego[5]

[1] Tufts University, Medford, MA 02155, USA
e-mail: anna.sajina@tufts.edu
[2] Haverford College, Haverford, PA 19041, USA
[3] National Radio Astronomy Observatory, Sorocco, NM 87891, USA
[4] Infrared Processing and Analysis Center, California Institute of Technology, Pasadena, CA 91125, USA
[5] Instituto de Física de Cantabria (CSIC-Universidad de Cantabria), Avda. los Castros s/n, 39005 Santander, Spain

Received 20 June 2012 / Accepted 13 November 2012

ABSTRACT

We report multiple epoch VLA/JVLA observations of 89 northern hemisphere sources, most with 37 GHz flux density >1 Jy, observed at 4.8, 8.5, 33.5, and 43.3 GHz. The high frequency selection leads to a predominantly flat spectrum sample, with 85% of our sources being in the *Planck* Early Release Compact Source Catalog (ERCSC). These observations allow us to: 1) validate *Planck*'s 30 and 44 GHz flux density scale; 2) extend the radio spectral energy distributions of *Planck* sources to lower frequencies allowing for the full 5−857 GHz regime to be studied; and 3) characterize the variability of these sources. At 30 GHz and 44 GHz, the JVLA and *Planck* flux densities agree to within ∼3%. On timescales of less than two months the median variability of our sources is 2%. On timescales of about a year the median variability increases to 14%. Using the WMAP 7-year data, the 30 GHz median variability on a 1−6 years timescale is 16%.

Key words. radio continuum: galaxies – galaxies: active – catalogs

1. Introduction

The *Planck* satellite (Planck Collaboration 2011a) is capable of all sky observation in nine bands ranging from 30 to 857 GHz. *Planck*'s primary goal is to make sensitive observations of temperature and polarization anisotropies in the cosmic microwave background (CMB), but it also offers unprecedented frequency coverage of both Galactic and extragalactic sources, as many of *Planck*'s bands lie in a frequency range at which accurate observations from the Earth's surface are very difficult due to atmospheric opacity. In addition, *Planck* has the ability to observe a given source at all frequencies essentially simultaneously, producing a wealth of spectral data much faster than ground based observatories can.

The first science product of *Planck* was the Early Release Compact Source Catalog (ERCSC; Planck Collaboration 2011b), which contains time-averaged flux densities of high reliability sources detected during the first year of *Planck*'s operation, including 1.6 full sky surveys.The majority of ERCSC sources are brighter than ∼0.5–1.0 Jy, though minimum intensity is also dependent on the frequency of observation. In the low frequency bands considered in this paper, the ERCSC contains hundreds of extragalactic radio sources (Planck Collaboration 2011b,c). These tend to be flat spectrum radio sources, predominantly blazars (Planck Collaboration 2011e; Giommi et al. 2011).

The photometric calibration of *Planck* is based on the large-scale dipole introduced by the solar motion relative to the cosmic microwave background, an approach unlike the calibration used by ground based observatories. This dipole is very well constrained, leaving a calibration uncertainty of ∼0.1%. However, the absolute flux density calibration on very small scales (e.g. for point sources) also depends on a precise knowledge of the *Planck* beam at a given frequency, which is less well constrained. Our current understanding of the beam solid angle suggests an uncertainty on the order of 1%. A cross-comparison of measured *Planck* and ground-based absolute flux density scales would therefore help either confirm that the adopted size of the *Planck* beam is within the expected uncertainty, or indicate that it may need further refinement. In addition, *Planck* provides a potential basis for future absolute flux density scales employed by ground-based facilities such as the Jansky Very Large Array (JVLA, formerly EVLA; Perley et al. 2011). To begin this process, an understanding of the current level of agreement between the two facilities is essential. Such a comparison, however, is complicated by the intrinsic variability of the sources that dominate the catalogs at the lowest *Planck* frequencies. This can be mitigated by observing as nearly simultaneously with *Planck* as possible, by using larger samples, and by better understanding of the intrinsic variability of the *Planck* sources.

In this paper, we present multiple-epoch VLA/JVLA observations of 89 sources in four spectral bands between 5 and 43 GHz, most of which are selected to be >1 Jy at 37 GHz, based on observations with the Metsähovi telescope (Hovatta et al. 2008, 2009). Preliminary results of this study were presented in Planck Collaboration (2011d). Based on 32 sources, a VLA-ERCSC flux density comparison found the median 30 GHz ERCSC flux density to be 8 ± 4% brighter than expected based on our VLA observations. Here we extend the previous analysis by including ∼3× more sources as well as using updated JVLA/VLA flux density standards. Unlike the case for our earlier paper, here we also have the advantage of multiple epoch observations of most sources that allow us to characterize the

⋆ Tables 3 and 4 are available in electronic form at http://www.aanda.org

intrinsic variability of the sources over a range of timescales. Our VLA/JVLA observations were all scheduled to be nearly simultaneous with the survey by survey *Planck* observations of the same sources, although here we only make comparisons with the time averaged ERCSC data which are publicly available.

Aside from our program, there have been two other programs involving near-simultaneous observations of *Planck*-detected radio sources[1]. The first of these programs was the PACO project, conducted in the southern hemisphere (Massardi et al. 2011), which observed 20 GHz-selected sources using the Australia Telescope Compact Array (ATCA). Sources were observed essentially simultaneously at 5.5, 9, 18, 21, 33 and 39 GHz. The second of these programs was SiMPlE, which followed-up 250 5 GHz-selected sources in the northern hemisphere using the single dish Medicina telescope at 5 and 8 GHz as well as at 21 GHz, with observations made between Aug. 2010 and Aug. 2011 (Procopio et al. 2011). Compared to these surveys, our work covers a smaller number of sources (89); however, our predominantly 37 GHz selection is most sensitive to the flat spectrum sources that dominate the *Planck*-detected radio sources. We use the JVLA whose *Ka* and *Q*-bands (33.45 and 43.22 GHz respectively) closely match *Planck*'s 28.46 and 44.10 GHz bands. These characteristics make our sample particularly well suited to the flux density comparison presented in this paper. The SiMPlE study is the only one using a single dish radio telescope, and hence has the advantage of providing accurate flux densities for extended sources. While all of these programs have their strengths and weaknesses, the intrinsic variability of the *Planck* radio sources means that ultimately the more such ancillary data is collected close in time to *Planck*'s observations of the same sources, the more value is added to the eventual *Planck* legacy point source catalog. Thanks to these three surveys, the vast majority of the brightest radio sources at ~5–40 GHz now have multiple epoch, near-simultaneous, ground-based observations. These observations extend the spectral energy distributions (SEDs) of the *Planck* detected blazars and flat spectrum radio galaxies to lower frequencies, and add data on the variability of these sources.

Our paper is organized as follows. In Sect. 2, we present the sample selection, observations, and data reduction. In Sect. 3.1 we present the cross-matching of our sample with the ERCSC. In Sect. 3.2, we analyze the SED types of our sources. In Sect. 3.3, we characterize their variability. In this section, we also make use of data from the Wilkinson Microwave Anisotropy Probe (WMAP; Bennett et al. 2003) to provide a longer timescale for our variability analysis. Finally, in Sect. 3.4, we compare the *Planck* and JVLA flux densities at 30 and 44 GHz. The summary and conclusions are presented in Sect. 4.

2. Data

2.1. VLA/JVLA sample

Our main goal in selecting galaxies for our survey was to observe as many sources that would be bright enough at the 30–40 GHz frequency range to have a high probability of being detected by the *Planck* Low Frequency Instrument (LFI; Mennella et al. 2011), which operates at frequencies of 30, 44, and 70 GHz. Our specific choice of VLA/JVLA observing targets was dictated by the goal of observing them as close to simultaneous with the *Planck* observations as possible.

The first results of our study presented in Planck Collaboration (2011d) included 32 sources chosen from the VLA calibrator list, where we specifically looked for 5 or 8 GHz flux densities >1 Jy. These published sources represent only the subset of the ones observed that were matched in the ERCSC at 30 GHz. In the present paper, we exclude the observations taken on July 24, 2009 since, for that day, we could not obtain primary flux calibrator measurements, but used a less reliable secondary calibrator. This leaves us with 23 of the sources in Planck Collaboration (2011d). We further include here data obtained on 16 sources in the same program on Nov. 15 and 18th, 2009, as well as on 11 more VLA sources that were not published in Planck Collaboration (2011d) because they did not have ERCSC counterparts.

In the present paper, we expand the sample with new JVLA data for 70 sources, which includes repeated observation of some of the above mentioned VLA sources. Our JVLA targets were predominantly selected from the Complete Northern 1 Jy Sample, which includes all 104 sources above declination −10° whose average 37 GHz flux density is >1 Jy, as determined through long-term 37 GHz monitoring by the Metsahovi telescope (e.g. Hovatta et al. 2008, 2009; Planck Collaboration 2011e)[2]. In this paper, while the analysis focuses on the sources with ERCSC counterparts, we publish the data for all sources we observed near simultaneously with *Planck* for the sake of upcoming *Planck* catalogs which will reach lower flux densities than the ERCSC. We still exclude from the analysis three sources for which we measure 33 GHz flux densities <300 mJy (these are cases where the wrong source was observed, or cases where the bulk of the flux is resolved out in our relatively high resolution imaging).

In summary, the sample we analyze includes 89 sources with a total of 159 separate observations. While the above makes it clear that the sample is neither homogeneous nor complete, 66 of our sources (~75 % of the total) are among the 104 in the Complete Northern 1 Jy Sample. These sources are therefore dominant, and largely determine the properties of our sample discussed in the rest of the paper. The spatial distribution of our sources can be seen in Fig. 1.

2.2. Observations

Our observations were made in two intervals of time, separated by approximately 6 months during which the NRAO array was down during the conversion from the VLA to the JVLA. In our earlier VLA observations, we used the *K* band detectors, centered at 22.46 GHz, whereas after the conversion to the JVLA, we switched to the *Ka* band (33.45 GHz). The *Ka* band is preferable to *K* band, because it is closer to *Planck*'s lowest frequency of 28.46 GHz, and also less affected by the atmospheric water vapor line at 22 GHz.

Observations were made in 23 observing blocks (Table 1)[3]. In the case of the JVLA observations, these were typically 1 h

[1] Like our program, these are not true follow up studies of *Planck*-detected sources, which cannot be done simultaneously with *Planck*'s observations, since *Planck* data reduction is time consuming. Instead, all three programs used their knowledge of *Planck*'s scanning strategy combined with known samples of bright radio sources to produce samples likely to heavily overlap with detections made by *Planck*.

[2] However, in instances where there were insufficient numbers of 37 GHz-selected sources to fill the required 1 h scheduling blocks (see Sect. 2.2) sources selected as above were used to fill in the block.

[3] For a few sources in our sample, we included earlier observations from Sajina et al. (2011) and, in the case of J0555+3948, earlier NRAO calibration observations (http://www.aoc.nrao.edu/~smyers/evlapolcal/polcal_master.html).

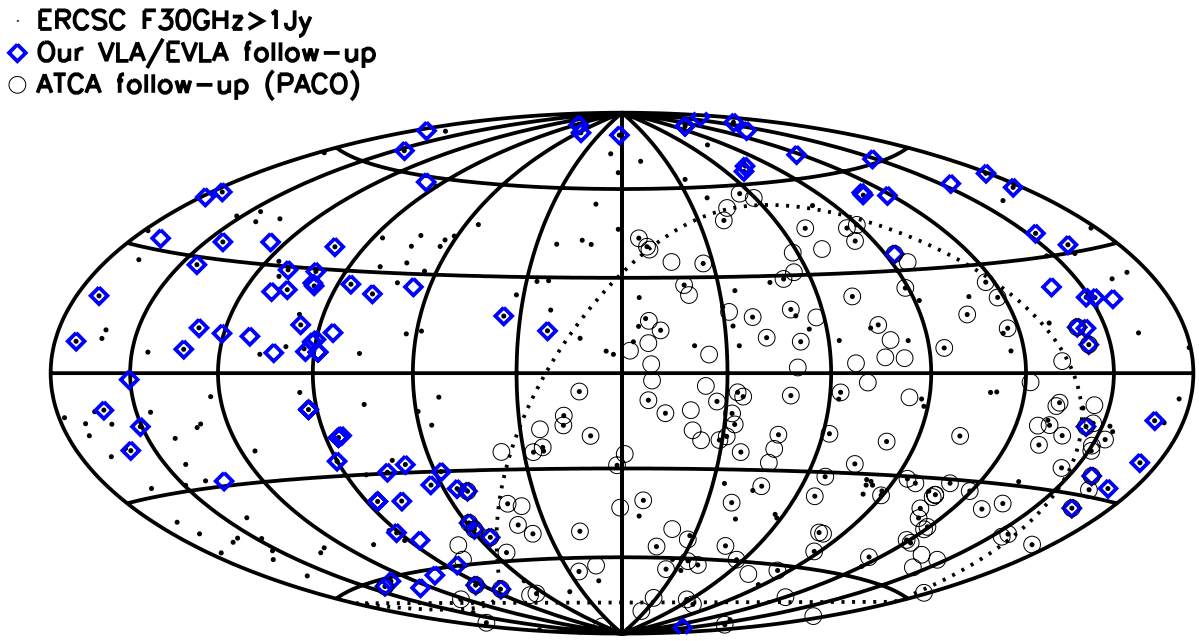

Fig. 1. Source map for the ERCSC and follow-up studies in Galactic coordinates. The dots mark positions of ERCSC 30 GHz sources at high Galactic latitude ($|b| > 5°$), with a >1 Jy cut applied, as at this level the sample is essentially complete. This is a total of 563 sources. Our study in the northern hemisphere includes 89 sources, the bulk of which are selected to have $S_{37\,\mathrm{GHz}} > 1$ Jy. For comparison, we plot the $S_{20\,\mathrm{GHz}} > 1$ Jy sources from the AT20G survey (Murphy et al. 2010) in the southern hemisphere. All of these are part of the PACO project, where sources >500 mJy make up the PACO bright sample (Massardi et al. 2011). A dotted line separates the sky into the region covered by our study and that covered by the PACO project. Altogether, in the >1 Jy regime, nearly 50% of the ERCSC 30 GHz sources have ground-based, near-simultaneous follow-up.

Table 1. Scheduling blocks with bands observed, dates, and array configuration.

Scheduling block	Bands observed	Date	Configuration
VLA 1	*C*, *X*, *K*, *Q*	Aug. 27, 2009	D
VLA 2	*C*, *X*, *K*, *Q*	Oct. 22, 2009	D
VLA 3	*C*, *X*, *K*, *Q*	Nov. 3, 2009	D
VLA 4	*C*, *X*, *K*, *Q*	Nov. 15, 2009	D
VLA 5	*C*, *X*, *K*, *Q*	Nov. 18, 2009	D
VLA 6	*C*, *X*, *K*, *Q*	Dec. 11, 2009	D
VLA 7	*C*, *X*, *K*, *Q*	Jan. 03, 2010	D
JVLA 1	*C*, *X*, *Ka*, *Q*	Jul. 2, 2010	D
JVLA 2	*C*, *X*, *Ka*, *Q*	Jul. 4, 2010	D
JVLA 3	*C*, *X*, *Ka*, *Q*	Jul. 9, 2010	D
JVLA 4	*C*, *X*, *Ka*, *Q*	Jul. 23, 2010	D
JVLA 5	*C*, *X*, *Ka*, *Q*	Aug. 3, 2010	D
JVLA 6	*C*, *X*, *Ka*, *Q*	Sep. 7, 2010	D
JVLA 7	*C*, *X*, *Ka*, *Q*	Sep. 15, 2010	D
JVLA 8	*C*, *X*, *Ka*, *Q*	Sep. 20, 2010	DnC
JVLA 9	*C*, *X*, *Ka*, *Q*	Sep. 24, 2010	DnC
JVLA 10	*C*, *X*, *Ka*, *Q*	Oct. 18, 2010	C
JVLA 11	*C*, *X*, *Ka*, *Q*	Oct. 20, 2010	C
JVLA 12	*C*, *X*, *Ka*, *Q*	Nov. 8, 2010	C
JVLA 13	*C*, *X*, *Ka*, *Q*	Nov. 9, 2010	C
JVLA 14	*C*, *X*, *Ka*, *Q*	Nov. 20, 2010	C
JVLA 15	*C*, *X*, *Ka*, *Q*	Nov. 27, 2010	C
JVLA 16	*C*, *X*, *Ka*, *Q*	Nov. 30, 2010	C

blocks. Each observing block included one of three standard calibrators (Table 2), as well as checks on array pointing, and 7−9 science targets. It is important to keep in mind that the bulk of these observations were done during very early stages of the JVLA's commissioning, when instrumental problems were to be anticipated. Given the brightness of our sources, even in the worst cases, the statistical error is below 0.5% (see Sect. 2.3 for details on observational errors and data flagging).

In all cases, the choice of specific targets to observe depended most strongly on the parts of the sky that the *Planck* satellite was scanning at the time of observation. With the queue-based system for JVLA scheduling, and given our higher demand for good weather, perfect simultaneity was not feasible. However, in the vast majority of cases, observations by *Planck* and the JVLA are separated by at most two weeks.

All of our observations were made with the VLA/JVLA array in its more compact configurations – D, C or DnC – where the angular resolution (the half power beam width) is 1−3″ at *K* band, 0.6−2″ at *Ka* band and 0.5−1.5″ at *Q* band[4] (22.46, 33.45, and 43.22 GHz respectively). With the exception of J1230+1223 (i.e. M 87), our sources were unresolved even at the highest frequency in the highest resolution configuration, so we can generally compare flux density measurements made in different configurations. In comparison, the *Planck* beam widths, as adopted in the ERCSC are 32.65′ at 30 GHz and 27.00′ at 44 GHz (Planck Collaboration 2011b).

2.3. Data reduction

Data reduction of the JVLA observations was done using the CASA software package[5]. We first performed all the standard initial reduction steps, including correction for atmospheric opacity, antenna delay solutions, and bandpass corrections. In addition, 15−20% of the raw data had to be removed before further analysis due to errors related to receiver malfunction, temporarily de-comissioned antennae (due to the ongoing transition from

[4] http://evlaguides.nrao.edu/index.php?title=Observational_Status_Summary_-_Current#Performance_of_the_JVLA

[5] http://www.casa.nrao.edu

Table 2. Flux densities of the primary JVLA calibrators.

Calibrator	RA	Dec	S_C (mJy)	S_X (mJy)	S_{Ka} (mJy)	S_Q (mJy)	C_C	C_X	C_K	C_Q
3C 048	01:37:41.2994	+33.09.35.1330	5437	3281	859	623	1.020	1.041	1.134	1.268
3C 286	13:31:08.2880	+30.30.32.9589	7394	5207	1893	1539	1.000	1.000	1.022	1.064
J0555+3948	05:55:30.8056	+39.48.49.1650	5339	4836	2681	2639	–	–	–	–

Notes. The listed correction values (C_C, C_X, C_K, and C_Q) given have been applied to the previously published VLA data (Planck Collaboration 2011d) and represent the ratio of the newer to the older flux density standards (see text for details).

VLA to JVLA), or time lapses in antenna slewing. Each source was amplitude and phase calibrated as well.

In each block, we included observations of one of three primary flux calibrators (Table 2), which provided the absolute flux density scale. We adopted the Perley-Butler 2010 absolute flux calibration standards. The VLA data originally presented in Planck Collaboration (2011d) were calibrated using the older Perley-Taylor 1999 standards, which we rescaled to the Perley-Butler 2010 flux standards. Table 2 gives the adopted calibrator flux densities, as well as the correction factors applied to the earlier VLA data.

After calibration, an image was produced for each observation. Each target source was fitted with a two dimensional gaussian providing peak and integrated flux densities as well as their associated errors. We checked for extended sources by looking for discrepancies between peak and integrated fluxes and by examination of images. We found one extended source, J1230+1223 (i.e. M 87, 3C 274). In Table 3 we present the integrated flux densities and flux density errors for each source, observation, and band. The flux density errors listed represent the quadrature sum of the errors from the above fitting, which are dominated by the instrumental noise in the images, and calibration uncertainties which are determined by the standard deviation of the flux densities of 3C 48 and 3C 286 (the primary flux calibrators) at each frequency. At the *Ka* and *Q* bands, the uncertainty introduced by the scatter in the measurements of the calibrators is estimated at ~0.1–0.2%.

2.4. The early release compact source catalog

In this paper, we obtain *Planck* flux densities for our sources from the *Planck* Early Release Compact Source Catalog (ERCSC; Planck Collaboration 2011b). The ERCSC contains high reliability (>90% cumulative reliability) compact sources (both Galactic and extragalactic) based on *Planck*'s first year of observations. In this paper, we adopt the standard flux density and flux density error estimates, as given in the FLUX and FLUX_ERR columns in the ERCSC catalogs. These are estimated through aperture photometry with a radius equal to the sky-averaged FWHM for the given band, with aperture corrections applied (Planck Collaboration 2011b). The ERCSC also includes flux density estimates based on fitting a 2D gaussian (GAUFLUX) as well as fitting the point-spread function PSFFLUX. The FLUX column is generally preferred since the GAUFLUX measurements are more sensitive to the presence of any underlying extended emission, while the PSFFLUX measure is affected by the fact that the exact shape of the *Planck* beam is not quite constant across the sky. In all cases, these flux densities are in fact averages of all data obtained for a given source by *Planck* observations at a given frequency. Since the ERCSC contains about 1.6 full sky surveys, the bulk of the sources have fluxes averaged over 2 or more time periods (with the sources closest to the ecliptic poles having the most frequent observations).

We note explicitly that the 44 GHz *Planck* measurements were generally noisier than those at 30 GHz. In addition, as discussed in Planck Collaboration (2011d), the placement of the three 44 GHz horns in the *Planck* focal plane ensured that there is an approximately one week separation in time between observations of a given source by one horn and the other two horns at that frequency. Thus variability is likely to play a larger role at 44 GHz than at 30 GHz, where the horn separation is smaller.

2.5. The WMAP 7-year data

The *WMAP* data used in this paper comes from the *WMAP* Seven Year release (Jarosik et al. 2011; Gold et al. 2011). The 7-year catalog contains 471 sources which represent 5σ peaks in the maps co-adding all data from the first 7 years of the survey in each of the 5 WMAP bands. The flux densities in this catalog are the mean flux densities of the sources across these 7 years. WMAP also produced single year maps, where (like the *Planck* observations) a given source has typically been observed more than once in the span of that year. Therefore even flux densities based on these single year maps are averaged over multiple observations. We obtain such yearly-averaged flux densities for the 471 sources in the 7-year catalog through the point source variability table[6]. Here we only make use of the WMAP *Ka* (30.0 GHz) data.

3. Results

3.1. Source matching

We consider a given JVLA-ERCSC source pair a match if the distance between them is less than 0.75 FWHM of the *Planck* beam for a given band. As seen in Fig. 2, the positional offsets for our matches never exceed ~6 arcmin and are typically within ~2 arcmin. Given the scarcity of extragalactic radio sources at the 1 Jy level, the chance of random association is negligible. However, in one case, the nominal *Planck* source is located in-between two of our sources (both listed as J1310+3220 in Table 3), and is the sum of the two. These sources are omitted from further analysis.

Of our 89 sources, we found 76 ERCSC matches at 30 GHz, and a subset of these (59) have ERCSC matches at 44 GHz (listed in Table 4). The typically negative 30–44 GHz spectral indices of our sources explain the lower number of matches at 44 GHz. This is also the result of the lower sensitivity of the *Planck* 44 GHz band, as mentioned in Sect. 2.4.

3.2. Sample characterization and SED types

Figure 3 shows a diagnostic color-color plot, providing an overview of the SEDs of our sources. It is obvious that our

[6] http://lambda.gfsc.nasa.gov/product/map/dr4/ptsrc_variability_info.cfm

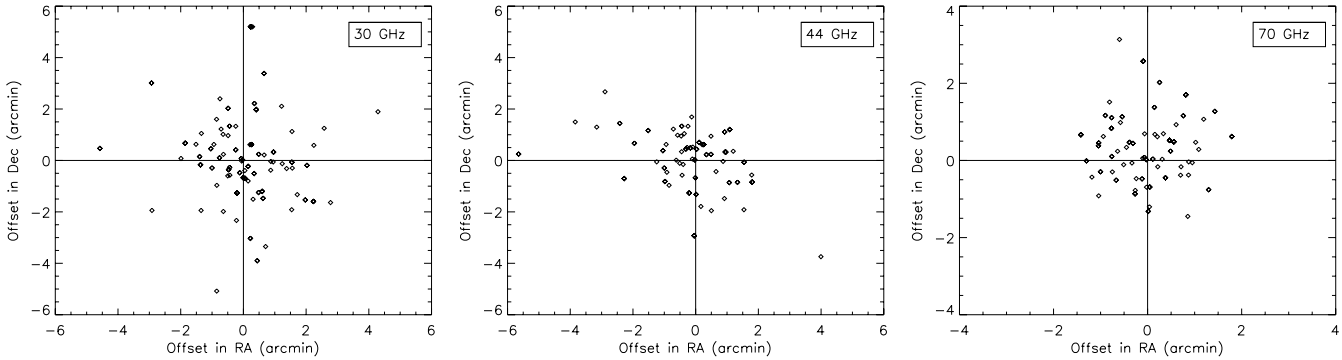

Fig. 2. Positional scatter between the Planck sources at 30, 44 GHz, and 70 GHz and their JVLA matches. For the 70 GHz comparison, the JVLA *Ka* positions are used.

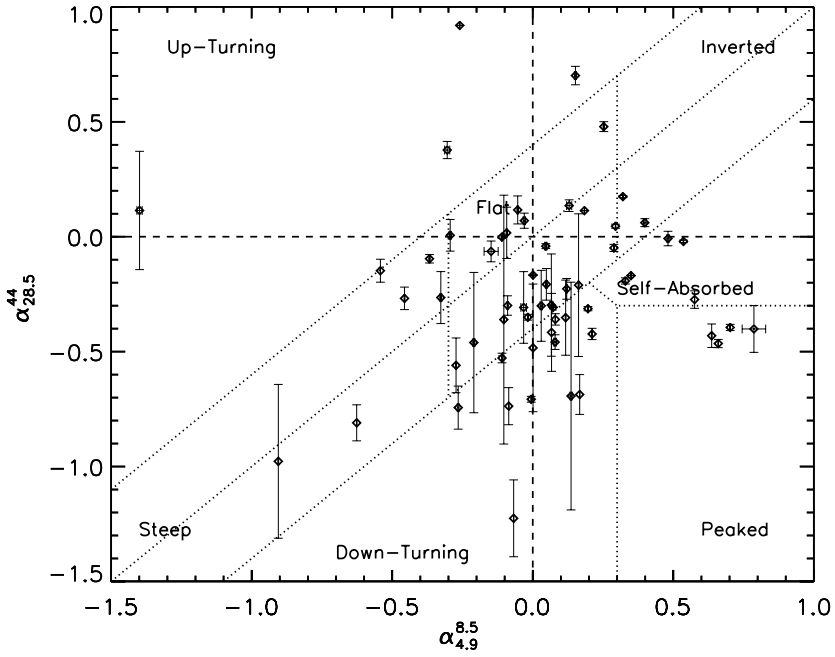

Fig. 3. 5–40 GHz radio source color–color diagnostic plot. Note that here we extrapolate both the VLA *K*-band and the JVLA *Ka*-band observations to 28.46 GHz, the center frequency of the *Planck* 30 GHz band. All observations for a given source are averaged, such that each data point represents a unique source. For ease of comparison, we adopt the Massardi et al. (2011) definitions of "flat", "steep", "up-turning", "inverted", "self-absorbed" and "peaked" spectra (as defined by the dotted regions).

Table 5. Relative frequency of different SED types, as defined in Fig. 3.

SED type	JVLA sample	PACO bright sample	PACO faint sample
Flat	42%	10%	5%
Steep	10%	4%	13%
Down turning	23%	66%	65%
Up turning	7%	0%	0%
Inverted	3%	1%	0%
Self absorbed	8%	5%	5%
Peaked	7%	15%	11%

Notes. Due to incomplete spectral coverage, this includes only 60 of our sources. The distribution of SED types for the PACO Bright and Faint samples are given for comparison (Massardi et al. 2011; Bonavera et al. 2011).

sample is biased toward flat-spectrum sources. In Table 5, we give the fractional distribution of each of the classes shown in Fig. 3, as well as the fractional composition of the PACO Bright and Faint samples (Massardi et al. 2011; Bonavera et al. 2011). We find that our sample has a much higher concentration of flat spectrum sources, compared with both PACO samples. This is unsurprising, given that the PACO selection is at 20 GHz, whereas our sample's primary selection is at 37 GHz. Naturally, the higher the frequency used to select a sample, the higher the fraction of flat spectrum relative to steep spectrum sources (e.g. Sajina et al. 2011). In addition, the PACO bright sample is based on $S_{20\ \mathrm{GHz}} > 0.5$ Jy, whereas ours has a threshold of

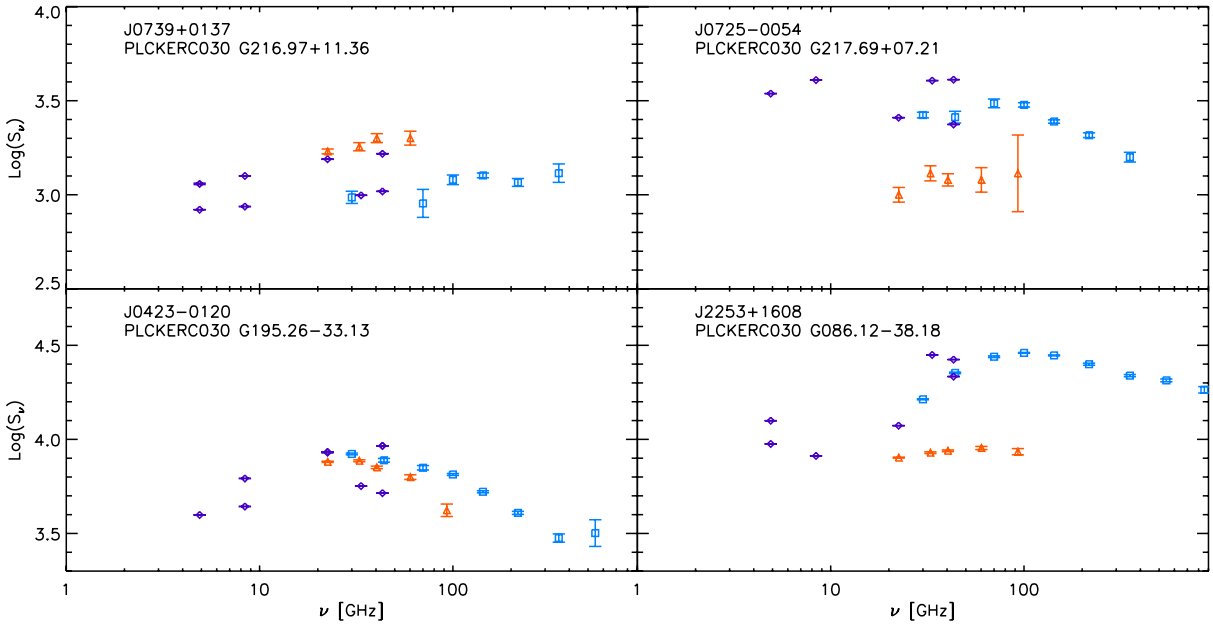

Fig. 4. The four most highly variable sources in our sample. The purple diamonds indicate VLA/JVLA data, orange triangles indicate the 7-year *WMAP* average flux densities of the sources, and light blue squares indicate the *Planck* ERCSC flux densities.

$S_{37\,\mathrm{GHz}} > 1$ Jy (for the ∼70% of the sample that are in the 1 Jy Complete Northern Sample). Adopting a typical spectral index[7] of −0.4, our flux density limit translates to 1.3 Jy at 20 GHz, brighter than the PACO bright sample limit.

As we demonstrate in Sect. 3.3, our sample shows significant variability. Four of the most highly variable sources are shown in Fig. 4, as an illustration. This variability means that a given source can be classified differently depending on when it is observed (both J0423-0120 and J2253+1608 clearly change the sign of their $\alpha^{44}_{28.5}$ from one observed epoch to the next). For simplicity, Fig. 3 is based on the average flux densities of our sources at each of the frequencies shown.

3.3. Variability analysis

The availability of multi-epoch observations allows us to study the variability of our sources, which is expected to be significant given that the bulk of our sample are flat spectrum sources, most likely blazars. For the variability analysis, we adopt the variability index formula from Sadler et al. (2006) which we reproduce in Eq. (1). In our implementation, we calculate the variability indices from pairs of observations, therefore $N = 2$ in Eq. (1). The variability is assessed on the basis of the *Ka* (33 GHz) flux densities from multiple observations of the same source. The available *K* (22 GHz) flux densities are included in the analysis, after being interpolated to the *Ka* central frequency using the $K - Q$ spectral indices.

$$V_{\mathrm{rms}} = \frac{100}{\langle S \rangle} \sqrt{\frac{\sum (S_i - \langle S \rangle)^2 - \sum \sigma_i^2}{N}}. \quad (1)$$

Time separations between pairs of VLA/JVLA observations are in the range of 1−450 days. To allow us to look for trends in variability at different time scales, we divide this roughly into three intervals that are big enough to include a statistically significant number of sources. These are: "Interval 1" which covers 0−60 days with a median of 12 days, "Interval 2" which covers 60−260 days with a median of 168 days, and "Interval 3" which covers 290−430 days with a median of 359 days. The number of sources included in each interval is ∼20. Variability is computed for each pair of observations, which are sorted into the appropriate interval depending on their time separation. The vast majority of sources have only 2 separate observations, if any. In the rare cases where a source has two pairs of observations in the same bin, the two values are averaged. Figure 5 shows the distributions of the variability indices for the different time intervals along with their median values. Note that since the availability and level of multiple epoch observations varies strongly from source to source, this is only representative of the entire sample under the assumption that sources with more repeated observation are not biased toward being more or less variable than sources with fewer repeat observations. This is generally true, with one exception. The most frequently observed sources are the two primary flux calibrators: 3C 48 (J0137+3309) and 3C 289 (J1331+3030). These sources are used as primary JVLA calibrators precisely because of their very low variability. To remove this bias, we also show the median variabilities with these two sources removed. As expected, the median variabilities are now larger.

A total of 68 of our sources (76% of the sample) have been detected by WMAP based on the 7-year data release. This allows us to sample a fourth, longest term interval, "Interval 4", which includes time separation of 1–6 years. We make use of the yearly averages for our sources as found in the WMAP 7 year *Ka* (30 GHz) data. The time separation between any pair of these varies between 1 and 6 years with a median value of ∼2.5 years. For the WMAP variability analysis, we apply Eq. (1) with $N = 7$.

Figure 5 shows that the median variability of sources increases with timescale from ∼3% within a few weeks to ∼14% from year-to-year, with the largest variability (∼16%) seen in the 1−7 year WMAP data. The fact that there is not a significant difference between our 1-year timescale variability and the 1−7 year WMAP variability estimate, is not surprising given that the median separation between the WMAP measurements is ∼2.5 years (see above), which is not a large enough separation for us to detect a significant change in the variability.

[7] Defined as $S \propto \nu^{\alpha}$.

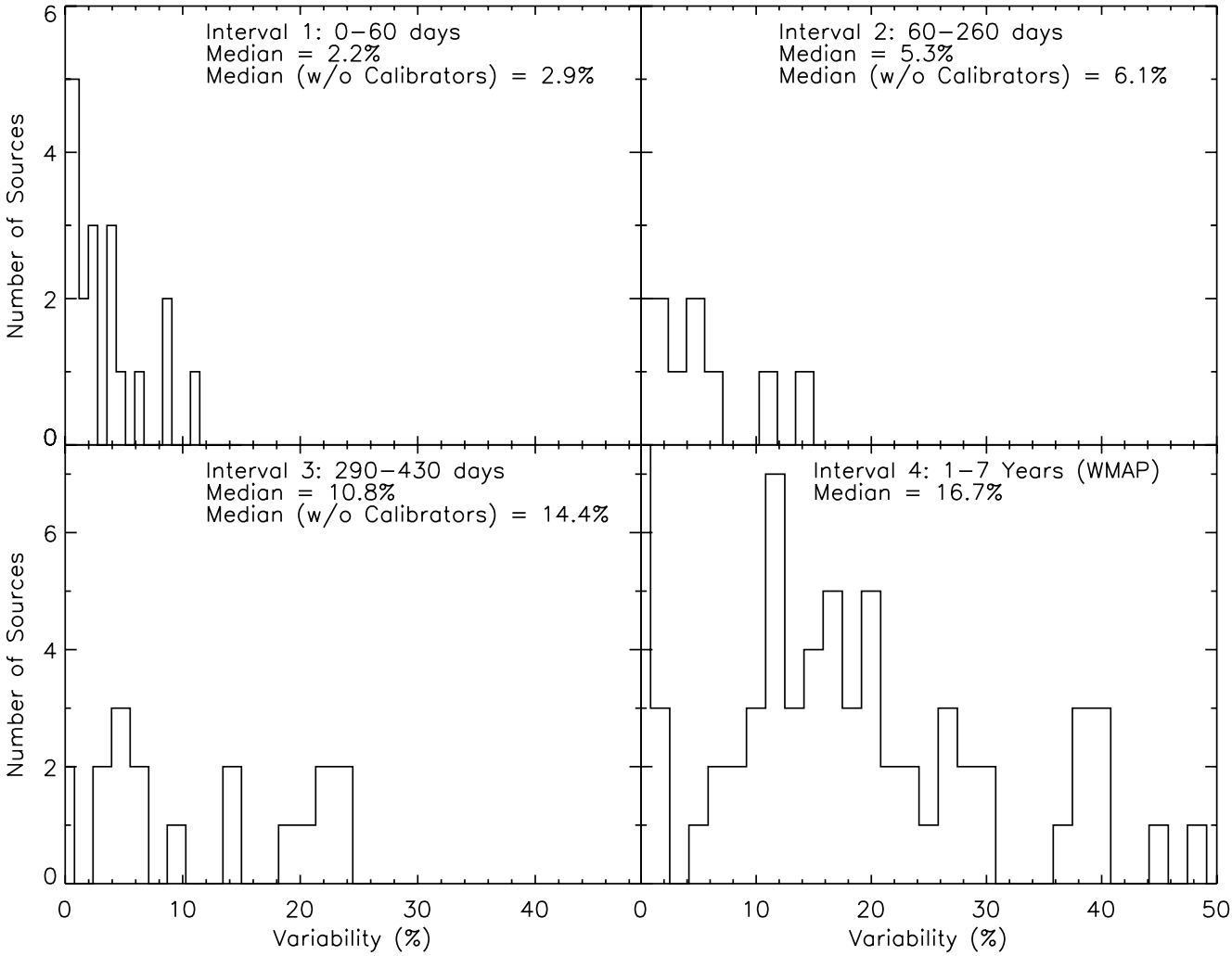

Fig. 5. Variability distribution on different timescales. The first three time intervals are based on our VLA/JVLA data alone. The last interval (1−7 years) is based on the yearly-averaged WMAP data (see text for details). All variability indices are estimated for the JVLA *Ka* band (33.5 GHz), or 33.0 GHz for WMAP.

We also repeated the analysis for the *C*-band (5 GHz) data to test how the variability of our sample changes with frequency as well as timescale. The results are summarized in Table 6. As expected, we found that the *C*-band variability is lower than at *Ka*, especially on the 1 year timescale where it is ∼3% at 5 GHz and 14% at 33 GHz.

The result that variability increases with frequency and timescale is consistent with the results found for the PACO bright sample (Massardi et al. 2011), although they only consider time intervals of 90, 180, and 270 days, whereas we also consider both shorter and longer timescales. They find that the 33 GHz median variability of their sources increases from 6.7 to 10.6% between 90 and 270 days, although dipping slightly to 6.3% at 180 days. The 90−270 day range is essentially our "Interval 2" in Fig. 5 where we find a median variability of 5.3% (after excluding the two calibrators). This is lower than the PACO-bright result, although, given the spread in Fig. 5, the two are marginally consistent. It is somewhat unexpected that PACO should find larger variabilities than we do, given that our sample includes more flat spectrum sources than the PACO-bright sample (see Table 5). The most likely explanation is that the variability index of a given source within a given time interval is based on the spread in flux densities around the mean flux density ($\langle S \rangle$ in Eq. (1)) for that particular time interval, whereas

Table 6. Median variability indices.

Band	0–60 days	60–260 days	290–430 days	1–7 years
5 GHz	1.0(1.1)	4.0(4.3)	3.0(3.3)	–
33 GHz	2.2(2.9)	4.0(5.3)	10.8(14.4)	15.6()

Notes. The values in parenthesis exclude the two calibrators 3C 48 and 3C 286.

Massardi et al. (2011) take the $\langle S \rangle$ to be the mean flux density based on all available observations of a given source. Given that variability increases with timescale, the quoted PACO variabilities are therefore likely to be biased high relative to ours. We choose to do our analysis in the manner described above, since: 1) the uneven time coverage of our data does not allow us to adopt equivalent "mean flux densities" for all sources; and 2) given the result that variability increases with time, adopting the mean flux density for a larger timescale than considered biases the estimated variability indices for a given interval. We refer the reader to Chen et al. (2012) for a much more detailed analysis of of the variability of the ERCSC sources based on WMAP data, including a discussion on the limitations of the commonly used variability index formula which we adopt here.

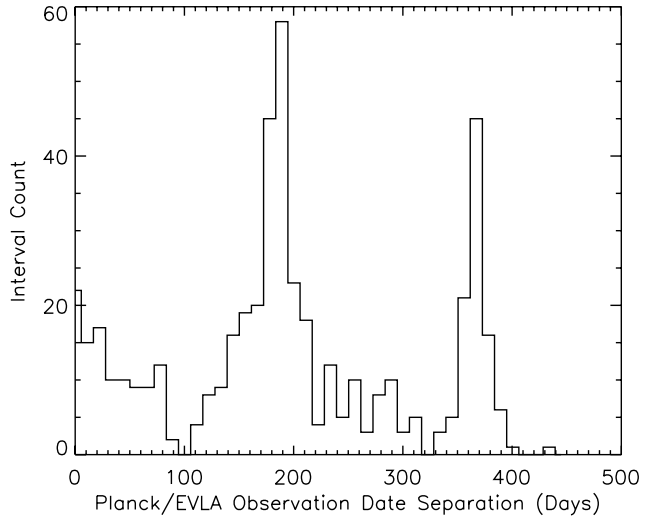

Fig. 6. Time intervals between our JVLA observations of a given source and the associated observations in the ERCSC. It is important to note that the bulk of our JVLA observations were actually taken after the end of period included in the ERCSC, but were timed so that in the majority of cases they were within a few weeks of the later *Planck* observations of the same source.

Lastly, Fig. 6 shows the distribution of time lags between ERCSC observations and each VLA/JVLA observation for the sources in our sample. The two most prominent peaks correspond to approximately six months and one year after the *Planck* observations included in the ERCSC. These arise because a typical source is revisited by *Planck* every six months. Our earlier VLA observations correspond to the time of *Planck*'s observations included in the ERCSC. Hence our later JVLA observations, done close in time to *Planck*'s observations of the same source, occur typically 6 months and then a year after the ERCSC observations. Given the above analysis, we expect the observed variability in comparing the ERCSC and VLA/JVLA observations to be ∼6−14%, as shown in Fig. 5 and Table 6.

3.4. JVLA-ERCSC flux density comparison

Here we compare the *Planck* ERCSC and JVLA flux density scales at 30 GHz and 44 GHz. Although our observations were scheduled to be close in time to *Planck* observations of the same sources, the comparison here is done against the public ERCSC and our survey extends about a year past the end of the period included in the ERCSC (see Fig. 6). In addition, the ERCSC itself includes data averaged over 1.6 sky surveys. Since we lack time ordered data from *Planck* for the time of the JVLA follow-up, and given the variability of our sources (see Sect. 3.3), individual source flux comparison is not meaningful. However, a *statistical* comparison can still be done. To do so, we extrapolate the *Ka* (*K*) ground-based flux densities to the *Planck* 30 GHz and 44 GHz bands (centered at 28.46 GHz and 44.1 GHz respectively). These extrapolations are done by assuming a power law between the *Ka* (or *K*) to *Q* bands with a spectral index as measured for each VLA/JVLA observation of a given source. We also apply color corrections to the *Planck* ERCSC flux densities. The multiplicative color corrections from the ERCSC Explanatory Supplement[8] are also based on the *Ka*-*Q* spectral index, but as measured from the ERCSC data, whenever both 30 and 44 GHz matches are found, or from the VLA/JVLA data otherwise.

As stated in Sect. 3.1, 76 of our sources have ERCSC 30 GHz matches and 59 have 44 GHz matches. For the flux density comparison, we exclude M 87 which is extended to the JVLA, as well as the two J1310+3220 sources which are blended in the ERCSC. Next, we exclude 8 sources whose WMAP variability index is >30%, as well as J0359+5057, which is very close to the Galactic plane ($b = -1.6°$) making its photometry less reliable. All other sources in the sample are sufficiently far from the Galactic plane (see Fig. 1) for Galactic emission to be negligible. Finally, we look for remaining outliers, i.e. sources whose ERCSC and JVLA flux densities are more than a factor of 2 discrepant. There are two such cases: J0418+3801 and J1751+0939. A literature search revealed that J0418+3801 (3C 111) is known to be a double lobed radio galaxy (Leahy et al. 1997). Our measurements are consistent with earlier VLA measurements of the core flux, but *Planck*'s much larger beam will respond to the extended structure resolved out in our interferometric observations. As for J1751+0939, our JVLA flux density measurements are below earlier data from both the VLA and WMAP. The source is variable, however, with a WMAP variability index just below our 30% cutoff mentioned above; therefore, it is possible that our observations were made at a time of particularly weak radio emission. Since our estimates at the four frequency bands are all consistent among themselves, it is less likely that this discrepancy is due to a mistake. We exclude J0418+3801 and J1751+0939 from the flux density comparison. This leaves us with a clean sample for the flux density comparison including 63 sources at 30 GHz and 49 sources at 44 GHz.

Figure 7 shows the 30 and 44 GHz JVLA-to-ERCSC flux density comparisons. Whenever applicable, we use the average flux densities based on all our VLA/JVLA observations of the same source. We next want to quantify the level of agreement between the JVLA and *Planck* ERCSC flux density scales. To minimize the possible effects of any remaining outliers, we compute the robust mean of each ratio, where 3σ outliers are excluded. At both 30 and 44 GHz, this removes just 2 sources. At 30 GHz, the robust mean of the *Planck*-to-JVLA ratio is 1.006 ± 0.026, while at 44 GHz it is 1.053 ± 0.040. In both cases, these values are clearly affected by Eddington bias (Eddington 1913) at the lower flux densities. To minimize this bias, we also compute the robust mean and median values for the sources where the extrapolated JVLA flux density is >1.5 Jy. With this flux density cut, no sources were excluded in the calculation of the robust mean. We find the robust mean(median) at 30 GHz is now 1.008(0.977) and at 44 GHz it is 0.983(0.993).

The above analysis suggests that the *Planck* ERCSC and (J)VLA flux densities are consistent with each other to within ∼2−3% at both 30 GHz and 44 GHz. This level of statistical agreement does not apply to individual sources, whose flux density uncertainties can be much larger. The best example is the primary (J)VLA flux density calibrator 3C 286 (J1331+3030), a well studied source with very low intrinsic variability. Compared to expectations from the JVLA, 3C 286 has a nearly 20% lower 30 GHz flux density in the ERCSC[9]. Only a 30% accuracy in the photometry is required for inclusion in the ERCSC, whose emphasis is on the reliability of the sources.

Figure 7 shows significant scatter, which is clearly larger than the nominal ERCSC flux density errors, which in turn are larger than the JVLA errors. Given the median variabilities on a

[8] http://irsa.ipac.caltech.edu/data/Planck/explanatory_supplement.pdf

[9] Although it is in agreement with expectations if the ERCSC's GAUFLUX value is used.

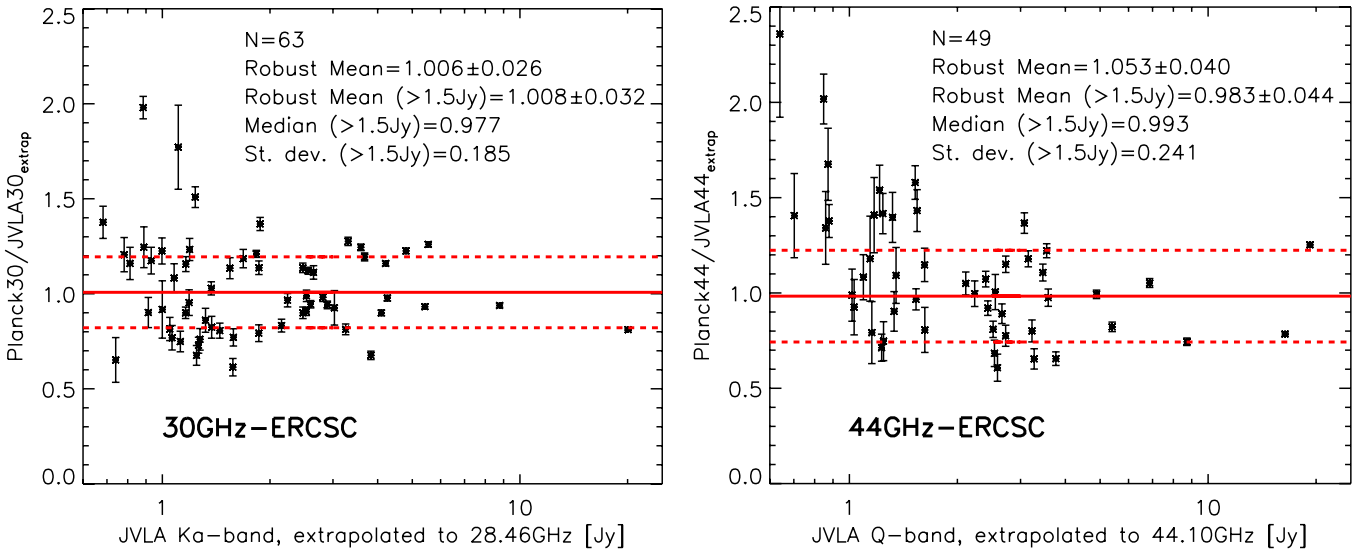

Fig. 7. Ratio of *Planck*-to-JVLA flux densities vs. JVLA flux densities at 30 (*left-hand panel*) and 44 GHz (*right-hand panel*). The *Planck* flux densities used are from the FLUX column of the ERCSC. The JVLA flux densities are extrapolated to the corresponding *Planck* central frequencies using the 33−43 GHz spectral index measured from the JVLA data. Some sources are excluded from this analysis, due to being extended, confused, or highly variable (see text for details). When multiple observations for a given source are available, these are averaged. Each panel shows the number of sources included, as well as the robust mean, median and standard deviations of the *Planck*-to-JVLA flux density ratios. To mitigate the effects of Eddington bias, we focus on the >1.5 Jy sources. The solid red lines show the median ratios for these sources, while the dashed red lines show the +/−1 standard deviation range.

∼6 months to a year timescale (see Fig. 5), we predict the scatter to be in the range 6−14%. This is lower than the measured standard deviation of 19%, which may be due to underestimated variability indices as well as additional flux density uncertainties. The nominal ERCSC flux density uncertainties are ∼3%, but including systematics they would have to be ∼15% to account for the observed scatter. This is within the discrepancy seen between the different flux density estimates (even within the ERCSC) for the essentially non-variable 3C 286.

As noted in Sect. 1, the accuracy of *Planck*'s calibration on small angular scales, including point sources, is determined by how well the *Planck* beam is known – in essence, the flux density scales as θ^2, where θ is the FWHM of the beam. Here we use the *Planck* flux density values as tabulated in the ERCSC, where the FWHM of the 30 GHz beam is 32.65 arcmin, and of the 44 GHz beam it is 27.00 arcmin. Work is ongoing to further refine our understanding of the *Planck* beams. Our results indicate that the *Planck* beams are unlikely to be revised by more than ∼2%, if we assume the JVLA flux density scale is completely accurate. If they are revised more significantly over time, this may indicate that it is the JVLA flux density scale that needs to be revised. Future work (Perley et al., in prep.) based on time ordered *Planck* data (which also include the observations presented here) will help further constrain the level of agreement between the two instruments.

4. Summary and conclusions

1. We present new 5, 8, 33, and 43 GHz observations for a sample of 89 bright (>70% selected to have $S_{37\,\mathrm{GHz}} > 1$ Jy) northern radio galaxies. Our observations were scheduled to be within a few weeks of the *Planck* coverage of these intrinsically variable sources, allowing for a range of studies including SED and variability analysis that shed light on the nature of the *Planck* detected radio sources. This study is complementary to similar work done in the southern hemisphere by the PACO project (e.g. Massardi et al. 2011; Bonavera et al. 2011) and in the northern hemisphere by the SiMPlE project (Procopio et al. 2011). Our study has the highest fraction of sources in the ERCSC (85%), thanks to its selection which favors higher flux density and flatter spectrum sources than PACO or SiMPLE.
2. From standard color–color diagnostic plots, we find that roughly 1/2 of our sources are flat-spectrum, 1/5 are steep spectrum, 1/5 are down-turning, and the remainder are up-turning, inverted, or self-absorbed. Examination of the 5−857 GHz SEDs shows that classification on the basis of two spectral indices is over simplistic and varies strongly depending on the frequency examined.
3. Multiple VLA/JVLA observations for nearly half the sources, along with archival WMAP data, allow us to assess the level of variability in bright radio galaxies on a range of timescales from several weeks to several years. We find that the median variability increases with timescale, from 3% (about 2 weeks) to 16% (about 2.5 years).
4. We compare the flux density scales for *Planck*'s two lowest-frequency LFI bands and the JVLA's *Ka* and *Q* bands. The agreement between the two instruments is within ∼2−3% at 30 GHz and 44 GHz. This is a significant improvement over previously reported results (Planck Collaboration 2011d), thanks to a larger sample, an improved JVLA flux density calibration, and better removal of the intrinsically most variable sources.

Acknowledgements. We are grateful to the anonymous referee for a careful reading of the paper and many useful suggestions which have improved the quality and presentation of the paper. We are particularly grateful to the *Planck* Collaboration for providing the public Early Release Compact Source Catalog (ERCSC). A description of the Planck Collaboration and a list of its members, including the technical or scientific activities in which they have been involved, can be found at http://www.sciops.esa.int/index.php?project=planck&page=Planck_Collaboration. This paper makes use of observations obtained at the Jansky Very Large Array (JVLA) which is an instrument of the National Radio Astronomy Observatory (NRAO). The NRAO is a facility of the National Science Foundation operated under cooperative agreement by Associated Universities, Inc. We are especially grateful to Leon Tavares for providing source lists of sources, drawn from the Complete Northern 1 Jy sample, to be observed by *Planck* in a given week. We are also grateful to

Charles Lawrence and Joaquin Gonzales-Nuevo for helpful discussions and reviews of the manuscript before submission. This work was funded through a subcontract to Tufts University, and another to Haverford College from NASA/JPL in support of *Planck* related activities. MLC acknowledges financial support from the Spanish MINECO projects AYA2010-21766-C03-01 and CSD2010-00064. The development of Planck has been supported by: ESA; CNES and CNRS/INSU-IN2P3-INP (France); ASI, CNR, and INAF (Italy); NASA and DoE (USA); STFC and UKSA (UK); CSIC, MICINN and JA (Spain); Tekes, AoF and CSC (Finland); DLR and MPG (Germany); CSA (Canada); DTU Space (Denmark); SER/SSO (Switzerland); RCN (Norway); SFI (Ireland); FCT/MCTES (Portugal); and The development of Planck has been supported by: ESA; CNES and CNRS/INSU-IN2P3-INP (France); ASI, CNR, and INAF (Italy); NASA and DoE (USA); STFC and UKSA (UK); CSIC, MICINN and JA (Spain); Tekes, AoF and CSC (Finland); DLR and MPG (Germany); CSA (Canada); DTU Space (Denmark); SER/SSO (Switzerland); RCN (Norway); SFI (Ireland); FCT/MCTES (Portugal); and PRACE (EU).

References

Bennett, C. L., Halpern, M., Hinshaw, G., et al. 2003, ApJS, 148, 1
Bonavera, L., Bonaldi, A., Massardi, M., et al. 2011, MNRAS, 416, 559
Eddington, A. S. 1913, MNRAS, 73, 359
Giommi, P., Polenta, G., Lahteenmaki, A., et al. 2012, A&A, 541, A160
Gold, B., Odegard, N., Weiland, J. L., et al. 2011, VizieR Online Data Catalog, 219, 20015
Hovatta, T., Nieppola, E., Tornikoski, M., et al. 2008, A&A, 485, 51
Hovatta, T., Valtaoja, E., Tornikoski, M., & Lähteenmäki, A. 2009, A&A, 494, 527
Jarosik, N., Bennett, C. L., Dunkley, J., et al. 2011, ApJS, 192, 14
Leahy, J. P., Black, A. R. S., Dennett-Thorpe, J., et al. 1997, MNRAS, 291, 20
Massardi, M., Bonaldi, A., Bonavera, L., et al. 2011, MNRAS, 415, 1579
Mennella, A., Butler, R. C., Curto, A., et al. 2011, A&A, 536, A3
Murphy, T., Sadler, E. M., Ekers, R. D., et al. 2010, MNRAS, 402, 2403
Perley, R. A., Chandler, C. J., Butler, B. J., & Wrobel, J. M. 2011, ApJ, 739, L1
Planck Collaboration 2011a, A&A, 536, A1
Planck Collaboration 2011b, A&A, 536, A7
Planck Collaboration 2011c, A&A, 536, A13
Planck Collaboration 2011d, A&A, 536, A14
Planck Collaboration 2011e, A&A, 536, A15
Procopio, P., Massardi, M., Righini, S., et al. 2011, MNRAS, 417, 1123
Sadler, E. M., Ricci, R., Ekers, R. D., et al. 2006, MNRAS, 371, 898
Sajina, A., Partridge, B., Evans, T., et al. 2011, ApJ, 732, 45

Pages 11 to 15 are available in the electronic edition of the journal at http://www.aanda.org

Table 3. VLA/JVLA source coordinates and flux densities.

Source	RA J2000	Dec J2000	Dateobs	S_C [mJy]	S_X [mJy]	S_{Ka} [mJy]	S_Q [mJy]
J0006-0623	1.5578871	–6.3931487	20100702	2415.0 ± 9.3	2301.6 ± 14.9	1653.4 ± 8.2	1369.1 ± 10.0
J0019+7327	4.9407767	73.4583381	20090827	1191.9 ± 0.7	1224.7 ± 1.4	*1051.2 ± 4.0	901.9 ± 6.2
J0050-0929	12.6721558	–9.4847806	20100723	254.1 ± 1.0	209.9 ± 1.4	123.7 ± 0.6	115.2 ± 0.9
J0108+0135	17.1615462	1.5834214	20100723	3558.8 ± 13.6	3909.3 ± 25.4	2736.1 ± 13.6	2295.3 ± 16.8
J0125-0005	21.3701825	–0.0988699	20100803	1263.6 ± 4.8	–	787.1 ± 3.9	649.7 ± 4.8
J0137+3309	24.4208333	33.1597222	20090827	5537.1 ± 0.1	3267.0 ± 0.1	*1234.9 ± 0.1	635.4 ± 0.1
J0137+3309	24.4220808	33.1597592	20091115	5543.7 ± 0.4	3280.7 ± 0.3	*1266.6 ± 5.7	667.1 ± 0.5
J0137+3309	24.4220808	33.1597592	20100702	5440.2 ± 20.8	3278.5 ± 21.3	858.1 ± 4.3	670.7 ± 4.9
J0137+3309	24.4220808	33.1597592	20100723	5438.7 ± 20.8	–	858.9 ± 4.3	669.5 ± 4.9
J0137+3309	24.4220808	33.1597592	20100803	5434.5 ± 20.8	–	858.1 ± 4.3	669.8 ± 4.9
J0137+3309	24.4220808	33.1597592	20100907	5428.6 ± 20.8	3279.9 ± 21.3	858.4 ± 4.3	670.6 ± 4.9
J0137+3309	24.4220808	33.1597592	20100920	5440.3 ± 21.0	–	858.8 ± 4.3	666.3 ± 4.9
J0137+3309	24.4220808	33.1597592	20100924	5431.0 ± 21.2	–	858.5 ± 4.3	684.7 ± 5.0
J0137+3309	24.4220808	33.1597592	20101020	5434.2 ± 21.2	–	860.7 ± 4.3	672.6 ± 5.0
J0137+3309	24.4220808	33.1597592	20101109	5392.7 ± 24.5	–	860.5 ± 4.5	672.7 ± 5.0
J0137+3309	24.4220808	33.1597592	20101120	5403.8 ± 21.9	–	858.9 ± 4.3	674.7 ± 5.0
J0137+3309	24.4220808	33.1597592	20101127	5385.6 ± 23.5	3316.1 ± 23.0	861.8 ± 4.4	674.0 ± 5.0
J0217+7349	34.3783892	73.8257283	20090827	4253.2 ± 1.0	4255.6 ± 4.2	*2974.5 ± 14.2	2169.1 ± 17.8
J0217+7349	34.3783892	73.8257283	20100920	3874.4 ± 14.9	–	2244.3 ± 11.1	1922.5 ± 14.1
J0217+7349	34.3783892	73.8257283	20100924	–	–	2284.8 ± 11.3	2284.6 ± 16.7
J0228+6721	37.2085479	67.3508415	20100920	1108.8 ± 4.3	–	903.6 ± 4.5	861.8 ± 6.3
J0319+4130	49.9506671	41.5116953	20100907	14 555.1 ± 56.1	21 103.0 ± 137.0	18 627.6 ± 92.4	16 539.0 ± 121.0
J0336+3218	54.1254483	32.3081507	20100907	–	2095.6 ± 13.6	2843.4 ± 14.1	2571.6 ± 18.8
J0359+5057	59.8739471	50.9639337	20100920	8834.3 ± 33.8	–	8246.9 ± 40.9	7162.9 ± 52.4
J0418+3801	64.5886542	38.0266111	20100920	2827.4 ± 19.6	–	2233.3 ± 11.1	2077.3 ± 15.2
J0423-0120	65.8125000	–1.3425000	20091103	–	–	*8505.0 ± 0.1	9245.7 ± 0.1
J0423-0120	65.8157917	–1.3426111	20091103	3966.9 ± 0.5	4398.9 ± 0.5	*8585.7 ± 0.6	9246.5 ± 0.6
J0423-0120	65.8158363	–1.3425181	20100907	–	6200.0 ± 40.2	5651.5 ± 28.0	5183.3 ± 37.9
J0433+0521	68.2962312	5.3543387	20100907	3225.1 ± 12.4	2765.8 ± 18.0	1539.1 ± 7.7	1333.7 ± 9.8
J0449+1121	72.2819629	11.3579435	20100907	1175.2 ± 4.5	1323.4 ± 8.6	1254.8 ± 6.2	1126.1 ± 8.2
J0449+1121	72.2819629	11.3579435	20100920	1161.5 ± 4.5	–	1248.4 ± 6.2	1173.3 ± 8.6
J0501-0159	75.3375000	–1.9872934	20100907	1037.5 ± 4.0	1158.7 ± 7.5	1497.5 ± 7.4	1382.2 ± 10.1
J0510+1800	77.5098713	18.0115505	2010920	–	–	565.3 ± 2.8	584.6 ± 4.3
J0530+1331	82.7350696	13.5319860	20100920	2191.4 ± 8.4	–	1119.8 ± 5.6	1098.3 ± 8.0
J0530+1331	82.7350696	13.5319860	20100924	2247.6 ± 8.6	–	1140.4 ± 5.7	1239.2 ± 9.1
J0541-0541	85.4086808	–5.6970634	20101130	2035.6 ± 1.0	1046.7 ± 1.0	582.0 ± 0.2	-
J0555+3948	88.8783567	39.8136569	20100301	5338.6	4835.9	2681.1	2639.4
J0555+3948	88.8783567	39.8136569	20100924	5199.3 ± 19.9	–	2453.9 ± 12.2	2461.5 ± 18.0
J0555+3948	88.8783567	39.8136569	20101018	5337.5 ± 0.3	–	2682.4 ± 0.7	2622.3 ± 1.7
J0555+3948	88.8783567	39.8136569	20101130	5069.1 ± 8.8	4738.7 ± 4.6	2681.1 ± 0.4	2635.9 ± 0.6
J0607-0834	91.9987467	–8.5805495	20100924	–	–	2237.8 ± 11.1	2235.1 ± 16.4
J0646+4451	101.6334417	44.8546084	20100924	–	–	2532.5 ± 12.6	2537.1 ± 18.6
J0721+7120	110.4727021	71.3434343	20101018	1738.2 ± 2.6	–	4024.2 ± 1.3	4251.5 ± 2.2
J0725-0054	111.4610000	–0.9156944	20091103	–	–	*2571.0 ± 0.1	2365.0 ± 0.1
J0725-0054	111.4610000	–0.9157068	20101018	3451.3 ± 1.7	4073.0 ± 0.5	4045.8 ± 1.2	4093.5 ± 0.7
J0738+1742	114.5308071	17.7052773	20101018	797.5 ± 1.8	784.1 ± 0.7	580.8 ± 0.3	591.2 ± 0.8
J0739+0137	114.8251408	1.6179494	20091022	1143.0 ± 10.0	1260.0 ± 1.3	*1546.7 ± 4.1	1652.8 ± 3.2
J0739+0137	114.8251412	1.6179494	20101018	833.7 ± 1.1	866.2 ± 0.4	993.6 ± 0.5	1042.9 ± 0.7
J0745-0044	116.4750000	–0.7380556	20091103	1970.0 ± 0.1	1964.0 ± 0.1	*960.0 ± 0.1	605.0 ± 0.1
J0750+1231	117.7166667	12.5177778	20091103	3685.0 ± 0.1	4486.0 ± 0.1	*4400.0 ± 0.1	3940.0 ± 0.1
J0750+1231	117.7168571	12.5180078	20101018	3750.8 ± 0.5	–	3079.0 ± 0.9	3002.3 ± 1.4
J0757+0956	119.2776667	9.9430278	20091022	1143.0 ± 6.0	1530.0 ± 1.2	*1903.2 ± 4.1	1964.7 ± 5.2
J0757+0956	119.2776787	9.9430145	20101018	1026.5 ± 0.3	1185.0 ± 1.2	1250.4 ± 0.4	1276.4 ± 1.3
J0808+4950	122.1652758	49.8434806	20091022	464.6 ± 0.9	454.0 ± 0.4	*488.0 ± 1.3	4220.6 ± 2.1
J0825+0309	126.4595833	3.1566667	20091022	776.9 ± 0.7	737.4 ± 0.6	*682.1 ± 3.5	689.7 ± 2.3
J0825+0309	126.4597433	3.1568111	20101108	559.6 ± 5.4	–	925.8 ± 2.4	1005.9 ± 1.1
J0830+2410	127.7170000	24.1833333	20091022	1269.0 ± 7.0	1246.0 ± 1.0	*1072.7 ± 5.1	877.4 ± 4.2
J0841+7053	130.3515417	70.8950556	20091022	1762.0 ± 9.0	1484.5 ± 0.8	*2267.0 ± 4.7	2900.0 ± 9.4
J0841+7053	130.3515221	70.8950481	20101018	1872.7 ± 0.6	–	2905.8 ± 0.9	2559.4 ± 1.5
J0854+2006	133.7036454	20.1085114	20101108	3531.4 ± 33.9	–	5997.9 ± 15.4	6803.7 ± 7.1
J0909+4253	137.3895833	42.8961389	20091118	1772.6 ± 0.6	1371.1 ± 1.1	*973.5 ± 1.6	817.1 ± 2.2
J0920+4441	140.2435771	44.6983292	20091118	1124.5 ± 0.4	1518.3 ± 1.0	*2475.3 ± 0.6	2393.0 ± 1.0
J0920+4441	140.2435771	44.6983292	20091118	1130.2 ± 0.5	1530.5 ± 0.6	*2478.5 ± 1.7	2495.2 ± 5.5
J0920+4441	140.2435771	44.6983292	20101108	1138.9 ± 10.9	–	2758.0 ± 7.1	3251.8 ± 3.5
J0927+3902	141.7625579	39.0391255	20091118	11 092.0 ± 3.5	11 846.0 ± 6.7	*9388.5 ± 40.9	7460.0 ± 31.9

Table 3. continued.

Source	RA J2000	Dec J2000	Dateobs	S_C [mJy]	S_X [mJy]	S_{Ka} [mJy]	S_Q [mJy]
J0927+3902	141.7625579	39.0391255	20101108	10 441.0 ± 100.8	–	9309.7 ± 23.9	9996.1 ± 10.5
J0948+4039	147.2305754	40.6623853	20091118	1656.3 ± 0.8	1563.0 ± 1.3	*1430.0 ± 20.0	1130.0 ± 10.0
J0948+4039	147.2305754	40.6623853	20101108	1772.0 ± 19.5	–	1151.7 ± 3.0	1293.9 ± 1.5
J0956+2515	149.2078142	25.2544583	20101108	667.0 ± 6.3	–	1230.9 ± 3.2	1316.2 ± 1.5
J0956+2515	149.2078142	25.2544583	20101130	642.6 ± 1.2	699.9 ± 0.8	1468.7 ± 0.2	1757.4 ± 0.6
J1038+0512	159.6949167	5.2080806	20100103	1233.0 ± 29.0	1920.0 ± 1.3	*1513.0 ± 3.5	1164.2 ± 3.6
J1043+2408	160.7876492	24.1431693	20101130	644.5 ± 0.2	742.9 ± 1.0	1149.2 ± 0.2	1299.0 ± 0.5
J1058+0234	164.6208333	2.5830556	20091103	–	–	*5985.0 ± 0.1	6344.0 ± 0.1
J1058+0133	164.6233542	1.5663333	20100103	3193.0 ± 7.0	4186.0 ± 3.0	*5431.9 ± 13.3	5404.0 ± 24.5
J1130+3815	172.7220000	38.2551389	20100103	1334.0 ± 2.0	1356.0 ± 1.0	*1041.0 ± 1.5	723.7 ± 3.6
J1130+3815	172.7220108	38.2551520	20101130	1370.6 ± 2.7	1538.7 ± 1.7	1327.8 ± 0.4	1319.5 ± 0.5
J1153+8043	178.3500000	80.7311111	20091103	–	–	*803.0 ± 0.1	642.0 ± 0.1
J1153+4931	178.3519583	49.5191194	20100103	1167.0 ± 1.2	949.0 ± 0.9	*904.1 ± 0.8	849.2 ± 2.4
J1159+2914	179.8791667	29.2452778	20091103	1609.0 ± 0.1	1530.0 ± 0.1	*1416.0 ± 0.1	1140.0 ± 0.1
J1159+2914	179.8826250	29.2455556	20100103	1609.0 ± 1.3	1530.0 ± 3.0	*1446.6 ± 4.1	1214.3 ± 9.6
J1221+2813	185.3820438	28.2329168	201074	446.6 ± 4.2	419.3 ± 2.2	326.7 ± 0.8	297.5 ± 0.4
J1222+0413	185.5939567	4.2210490	20100704	783.7 ± 7.4	1076.3 ± 5.7	1000.8 ± 2.6	903.6 ± 1.1
J1222+0413	185.5939567	4.2210490	20100709	782.8 ± 7.4	1089.7 ± 5.7	1063.5 ± 2.7	1021.7 ± 1.1
J1224+2122	186.2271250	21.3797222	20100103	1233.0 ± 2.0	1267.0 ± 1.4	*1442.5 ± 4.1	1260.0 ± 8.5
J1229+0203	187.2779154	2.0523884	20100704	37 172.1 ± 360.1	31 724.1 ± 187.0	22 899.1 ± 59.9	19 226.6 ± 24.5
J1229+0203	187.2779154	2.0523884	20100709	37 738.1 ± 357.1	32 793.1 ± 173.6	24 318.3 ± 62.4	19 812.5 ± 20.3
J1230+1223	187.7059308	12.3911233	20100704	53 260.1 ± 548.8	24 892.1 ± 163.9	1669.4 ± 14.2	1807.8 ± 7.7
J1230+1223	187.7059308	12.3911233	20100709	59 530.1 ± 719.9	26 430.1 ± 177.1	1913.7 ± 13.5	1884.1 ± 5.0
J1310+3220	197.6194167	32.3455000	20100103	1427.0 ± 1.7	2133.0 ± 1.4	*2917.7 ± 5.1	2125.2 ± 16.0
J1310+3220	197.6194325	32.3454953	20100709	1963.4 ± 18.5	2718.1 ± 14.3	2548.0 ± 6.5	2312.3 ± 2.4
J1327+2210	201.7535879	22.1806010	20100709	1856.9 ± 17.5	1746.1 ± 9.2	1232.9 ± 3.2	1077.2 ± 1.1
J1331+3030	202.7845333	30.5091553	20091118	7481.4 ± 0.6	5202.6 ± 0.5	*2574.5 ± 1.6	1557.1 ± 0.5
J1331+3030	202.7845333	30.5091553	20100103	7485.0 ± 0.5	5202.3 ± 0.4	*2570.4 ± 0.3	1532.5 ± 0.3
J1331+3030	202.7845333	30.5091553	20100704	7398.4 ± 69.8	5200.4 ± 27.3	1890.9 ± 4.9	1530.3 ± 1.7
J1331+3030	202.7845333	30.5091553	20100709	7387.3 ± 69.7	5243.5 ± 27.5	1891.3 ± 4.9	1531.1 ± 1.6
J1331+3030	202.7845333	30.5091553	20100915	7382.4 ± 69.7	5251.5 ± 27.6	1898.6 ± 4.9	1533.8 ± 1.7
J1331+3030	202.7845333	30.5091553	20101108	7251.2 ± 68.7	–	1892.2 ± 4.9	1532.6 ± 1.6
J1419+5423	214.9441667	54.3872222	20100103	1178.0 ± 1.6	1249.0 ± 7.0	*1257.6 ± 1.6	1251.5 ± 4.3
J1419+5423	214.9441558	54.3874409	20100704	1097.6 ± 10.4	1096.9 ± 5.8	963.6 ± 2.5	949.8 ± 1.1
J1419+5423	214.9441558	54.3874409	20100709	1063.2 ± 10.1	1081.2 ± 5.7	909.7 ± 2.3	893.3 ± 0.9
J1642+6856	250.5327021	68.9443768	20100704	2520.8 ± 23.8	2617.4 ± 13.7	1696.2 ± 4.9	1524.8 ± 2.1
J1642+6856	250.5327021	68.9443768	20100709	2482.9 ± 23.4	–	1735.3 ± 4.5	1567.7 ± 1.6
J1728+1215	262.0293800	12.2609683	2010915	–	464.8 ± 2.4	451.8 ± 1.2	425.5 ± 0.5
J1743-0350	265.9952337	–3.8346158	20100915	3316.3 ± 31.3	3469.5 ± 18.2	3616.1 ± 9.3	3298.0 ± 3.5
J1751+0939	267.8867442	9.6502024	20100915	1619.8 ± 15.3	1905.7 ± 10.0	2111.2 ± 5.5	2085.1 ± 2.2
J1800+3848	270.1031892	38.8085271	20100915	–	–	551.6 ± 1.4	504.8 ± 0.6
J1800+7828	270.1903496	78.4677829	20101020	2497.1 ± 9.6	–	2522.4 ± 12.5	2515.8 ± 18.4
J1806+6949	271.7111692	69.8244746	20100704	1537.1 ± 14.7	1478.1 ± 7.8	1202.0 ± 3.5	1185.5 ± 1.9
J1806+6949	271.7111692	69.8244746	20100709	1524.5 ± 14.6	1481.1 ± 7.8	1235.2 ± 3.4	1192.5 ± 1.8
J1806+6949	271.7111692	69.8244746	20101109	1383.4 ± 6.4	–	1241.0 ± 6.3	1296.0 ± 9.5
J1806+6949	271.7111692	69.8244746	20101127	1440.8 ± 6.3	1409.2 ± 10.3	1058.7 ± 5.3	1231.3 ± 9.1
J1824+5651	276.0294517	56.8504141	20100915	–	1362.2 ± 7.2	1137.2 ± 3.1	1096.9 ± 1.4
J1829+4844	277.3824300	48.7461558	20100915	5042.5 ± 47.6	3716.4 ± 19.5	2498.6 ± 6.8	2405.8 ± 4.4
J1849+6705	282.3169679	67.0949111	20100723	1434.7 ± 5.5	2152.3 ± 14.0	2720.4 ± 13.5	2473.9 ± 18.1
J1849+6705	282.3169679	67.0949111	20100803	1452.0 ± 5.7	–	2979.9 ± 14.8	2861.2 ± 20.9
J1849+6705	282.3169679	67.0949111	20100915	1395.9 ± 13.2	2050.6 ± 10.8	2463.8 ± 6.3	2212.1 ± 2.3
J1849+6705	282.3169679	67.0949111	20101020	–	–	2252.6 ± 11.2	2349.2 ± 17.2
J1849+6705	282.3169679	67.0949111	20101109	1259.9 ± 5.0	–	2247.8 ± 11.2	2295.2 ± 16.8
J1927+7358	291.9520633	73.9671028	20101020	–	–	4446.9 ± 22.2	4851.7 ± 35.5
J1955+5131	298.9280763	51.5301517	20101020	–	–	1333.4 ± 6.6	1589.4 ± 11.6
J1955+5131	298.9280763	51.5301517	20101120	1296.5 ± 5.7	–	1267.8 ± 6.3	1127.7 ± 8.3
J1955+5131	298.9280763	51.5301517	20101127	1326.8 ± 5.9	1387.5 ± 9.2	1141.8 ± 5.7	1015.4 ± 7.4
J2005+7752	301.3791604	77.8786799	20101020	924.7 ± 3.6	–	689.6 ± 3.4	701.0 ± 5.2
J2007+4029	301.9372704	40.4968345	20091115	2956.5 ± 3.1	3810.3 ± 1.9	*3141.2 ± 14.7	2465.4 ± 20.3
J2007+4029	301.9372704	40.4968345	20101020	3534.2 ± 13.6	–	3506.0 ± 17.4	3949.9 ± 29.0
J2022+6136	305.5278404	61.6163346	20100702	3161.5 ± 12.1	3058.8 ± 19.9	1136.0 ± 5.6	839.6 ± 6.1
J2022+6136	305.5278404	61.6163346	20100723	3227.4 ± 12.4	3089.9 ± 20.1	1134.5 ± 5.6	819.8 ± 6.0
J2022+6136	305.5278404	61.6163346	20100803	3242.4 ± 12.4	–	1213.7 ± 6.0	1027.5 ± 7.5
J2053+5427	313.4791667	54.4597222	20091103	2850.0 ± 0.1	3311.0 ± 0.1	*2460.0 ± 0.1	1360.0 ± 0.1
J2123+0535	320.9354892	5.5894703	20091115	2168.4 ± 4.0	1927.0 ± 2.0	*1144.8 ± 6.5	847.5 ± 9.3
J2123+0535	320.9354892	5.5894703	20101109	2564.6 ± 10.9	–	1421.1 ± 7.1	1550.6 ± 11.3

Table 3. continued.

Source	RA J2000	Dec J2000	Dateobs	S_C [mJy]	S_X [mJy]	S_{Ka} [mJy]	S_Q [mJy]
J2133+1443	323.4057888	14.7295753	20101109	164.5 ± 0.7	–	133.7 ± 0.7	118.6 ± 0.9
J2134-0153	323.5429583	–1.8881111	20091103	–	–	*1925.5 ± 0.1	1545.0 ± 0.1
J2134-0153	323.5429583	–1.8881111	20091115	2450.2 ± 5.4	2492.0 ± 2.7	*2089.5 ± 10.1	1717.1 ± 14.6
J2136+0041	324.1607762	0.6983926	20091115	–	8334.4 ± 35.4	*4367.0 ± 27.2	2536.1 ± 26.3
J2136+0041	324.1607762	0.6983926	20101109	9412.6 ± 36.8	–	4968.0 ± 24.7	5028.3 ± 36.8
J2139+1423	324.7554554	14.3933311	20091115	2986.9 ± 5.0	3202.7 ± 2.1	*2080.3 ± 9.3	1294.1 ± 14.7
J2139+1423	324.7554554	14.3933311	20101120	2930.4 ± 11.9	–	2015.1 ± 10.0	1595.0 ± 11.7
J2139+1423	324.7554554	14.3933311	20101127	2987.5 ± 11.7	3345.4 ± 21.8	1613.0 ± 8.0	1726.4 ± 12.6
J2148+0657	327.0227500	6.9607222	20091115	5356.3 ± 15.3	5559.4 ± 7.6	*3852.2 ± 27.2	3172.3 ± 33.0
J2148+6107	327.0668558	61.1182883	20090827	1224.7 ± 0.6	996.1 ± 1.3	*601.1 ± 2.5	330.0 ± 4.2
J2202+4216	330.6804167	42.2775000	20091103	3994.0 ± 0.1	3996.0 ± 0.1	*3440.0 ± 0.1	3085.0 ± 0.1
J2203+3145	330.8124167	31.7606389	20091103	2165.0 ± 0.1	2495.0 ± 0.1	*2576.0 ± 0.1	2841.0 ± 0.1
J2203+3145	330.8123992	31.7606305	20100702	1997.6 ± 8.3	2515.4 ± 16.3	2864.1 ± 14.2	2500.8 ± 18.3
J2203+1725	330.8620417	17.4300556	20091103	987.0 ± 0.1	1055.0 ± 0.1	*1035.0 ± 0.1	1073.0 ± 0.1
J2203+1725	330.8620571	17.4300688	20101120	937.2 ± 4.6	–	1573.3 ± 7.8	1271.6 ± 9.3
J2203+1725	330.8620571	17.4300688	20101127	893.4 ± 3.6	1197.2 ± 7.8	1558.5 ± 7.7	1663.6 ± 12.2
J2218-0335	334.7168333	–3.5935833	20091115	2254.1 ± 3.9	1875.0 ± 1.6	*1214.3 ± 4.8	1021.5 ± 8.2
J2225-0457	336.4469167	–4.9503889	20091115	7219.7 ± 16.0	7795.0 ± 5.0	*5656.0 ± 24.0	3597.0 ± 26.0
J2229-0832	337.4170417	–8.5484722	20091115	2085.4 ± 4.5	1767.6 ± 1.2	*1234.3 ± 5.4	1239.3 ± 9.3
J2230+6946	337.6519571	69.7744658	20090827	743.1 ± 0.4	748.2 ± 0.9	*572.7 ± 3.3	405.9 ± 3.7
J2232+1143	338.1517083	11.7308056	20091103	5594.0 ± 0.1	5827.0 ± 0.1	*4407.0 ± 0.1	3606.0 ± 0.1
J2236+2828	339.0936250	28.4826111	20091103	1285.0 ± 0.1	1273.0 ± 0.1	*1412.0 ± 0.1	1547.0 ± 0.1
J2236+2828	339.0936287	28.4826148	20100702	1595.7 ± 6.1	1434.7 ± 9.3	1595.7 ± 7.9	1541.4 ± 11.3
J2253+1608	343.4906250	16.1482222	20091103	9463.0 ± 0.1	8176.0 ± 0.1	*11834.0 ± 0.1	21 570.1 ± 0.1
J2253+1608	343.4906162	16.1482114	20100702	12 572.6 ± 48.2	–	28 126.0 ±139.5	26 563.1 ± 194.2
J2316+1618	349.1654112	16.3018731	201072	246.1 ± 1.0	198.1 ± 1.3	139.3 ± 0.7	129.6 ± 1.0
J2327+0940	351.8899192	9.6692952	20100702	1024.9 ± 3.9	1002.9 ± 6.5	990.4 ± 4.9	891.8 ± 6.5
J2327+0940	351.8899192	9.6692952	20100723	1010.1 ± 3.9	1012.2 ± 6.6	1123.2 ± 5.6	1040.7 ± 7.6
J2327+0940	351.8899192	9.6692952	20100803	998.8 ± 3.8	–	1317.3 ± 6.5	1300.0 ± 9.5
J2354+4553	358.5903346	45.8845101	20100723	1260.0 ± 4.8	1012.9 ± 6.6	492.5 ± 2.4	399.5 ± 2.9
J2354+4553	358.5903346	45.8845101	20100803	1280.6 ± 4.9	–	500.7 ± 2.5	409.8 ± 3.0

Notes. The errors include statistical error as well as calibration uncertainty. (*) Observations marked with * are VLA observations done at *K* (22 GHz) instead of *Ka* (33 GHz).

Table 4. Matches of our VLA/JVLA sources with sources in the ERCSC catalog.

J2000 name	*Planck* name	(J)VLA dateobs	Planck dateobs
J0006-0623	PLCKERC030 G093.49-66.62	20100702	20091221
J0108+0135	PLCKERC030 G131.82-60.99	20100723	20100112
J0125-0005	PLCKERC030 G141.26-61.77	20100803	20100115, 20100116
J0137+3309	PLCKERC030 G133.94-28.63	20100702, 20100723, 20100803, 20100907, 20100920, 20100924, 20101020, 20101109, 20101127, 20101120, 20091115, 20090827	20100130, 20100131
J0217+7349	PLCKERC030 G128.95+11.97	20100920, 20100924, 20090827	20090911, 20090912, 20100219, 20100220
J0228+6721	PLCKERC030 G132.15+06.22	20100920	20090906, 20100217, 20100218
J0319+4130	PLCKERC030 G150.59-13.25	20100907	20090829, 20100218, 20100219
J0336+3218	PLCKERC030 G159.01-18.79	20100907	20090828, 20090829, 20100220
J0359+5057	PLCKERC030 G150.36-01.65	20100920	20090907, 20090908, 20100225
J0418+3801	PLCKERC030 G161.66-08.78	20100920	20090906, 20090907, 20100227, 20100228
J0423-0120	PLCKERC030 G195.26-33.13	20100907, 20091103, 20091103	20090828, 20090829, 20100226, 20100227
J0433+0521	PLCKERC030 G190.40-27.42	20100907	20090901, 20100301
J0449+1121	PLCKERC030 G187.35-20.74	20100907, 20100920	20090906, 20100303
J0501-0159	PLCKERC030 G201.45-25.29	20100907	20090905, 20090906, 20100305
J0530+1331	PLCKERC030 G191.42-11.03	20100920, 20100924	20090914, 20090915, 20100310, 20100311
J0555+3948	PLCKERC030 G171.66+07.28	20100301, 20100924, 20101018, 20101130	20090922, 20100313, 20100314
J0607-0834	PLCKERC030 G215.75-13.51	20100924	20090919, 20090920, 20100322, 20100323
J0646+4451	PLCKERC030 G171.09+17.92	20100924	20090930, 20091001, 20100322
J0721+7120	PLCKERC030 G143.98+28.03	20101018	20091005, 20100317, 20100318
J0725-0054	PLCKERC030 G217.69+07.21	20101018, 20091103	20091009, 20091010, 20100407
J0738+1742	PLCKERC030 G201.84+18.14	20101018	20091010, 20091011, 20100406
J0739+0137	PLCKERC030 G216.97+11.36	20101018, 20091022	20091012, 20091013, 20100409, 20100410
J0745-0044	PLCKERC030 G219.91+11.78	20091103	20091014, 20091015, 20100411, 20100412
J0750+1231	PLCKERC030 G208.18+18.75	20091103, 20101018	20091014, 20100410
J0757+0956	PLCKERC030 G211.33+19.05	20101018, 20091022	20091016, 20100411, 20100412
J0825+0309	PLCKERC030 G221.26+22.36	20101108, 20091022	20091024, 20091025, 20100419, 20100420
J0830+2410	PLCKERC030 G200.06+31.89	20091022	20091021, 20100415, 20100416
J0841+7053	PLCKERC030 G143.55+34.41	20101018, 20091022	20091012, 20100326, 20100327
J0854+2006	PLCKERC030 G206.78+35.81	20101108	20091027, 20100421, 20100422
J0909+4253	PLCKERC030 G178.32+42.86	20091118	20091024, 20100417
J0920+4441	PLCKERC030 G175.71+44.81	20091118, 20091118, 20101108	20091025, 20100418, 20100419
J0927+3902	PLCKERC030 G183.72+46.16	20091118, 20101108	20091028, 20100422, 20100423
J0948+4039	PLCKERC030 G181.02+50.31	20091118, 20101108	20091031, 20100426, 20100427
J0956+2515	PLCKERC030 G205.49+50.96	20101108, 20101130	20091108, 20100505
J1043+2408	PLCKERC030 G211.59+61.00	20101130	20091119, 20091120, 20100519
J1058+0133	PLCKERC030 G251.59+52.70	20100103	20091207, 20091208, 20100601, 20100602
J1130+3815	PLCKERC030 G174.47+69.79	20101130, 20100103	20091121, 20100527
J1153+4931	PLCKERC030 G145.58+64.96	20100103	20091116, 20091117, 20100525, 20100526
J1153+8043	PLCKERC030 G125.75+35.85	20091103	20091016, 20091017, 20100321, 20100322
J1159+2914	PLCKERC030 G199.42+78.39	20100103, 20091103	20091204, 20091205
J1222+0413	PLCKERC030 G284.63+66.05	20100704, 20100709	20091229, 20091230
J1224+2122	PLCKERC030 G255.00+81.65	20100103	20091218, 20091219
J1229+0203	PLCKERC030 G290.02+64.36	20100704, 20100709	20100102
J1230+1223	PLCKERC030 G283.75+74.54	20100704, 20100709	20091226, 20091227
J1310+3220	PLCKERC030 G085.86+83.31	20100709, 20100103	20091221, 20091222
J1327+2210	PLCKERC030 G003.62+80.50	20100709	20100105, 20100106
J1331+3030	PLCKERC030 G056.70+80.65	20100704, 20100709, 20100915, 20101108, 20091118, 20100103	20091230, 20091231
J1419+5423	PLCKERC030 G098.28+58.29	20100704, 20100709, 20100103	20091206, 20091207
J1642+6856	PLCKERC030 G100.69+36.62	20100704, 20100709	20091106, 20091107, 20091108, 20100222, 20100223, 20100224,

Table 4. continued.

J2000 name	*Planck* name	(J)VLA dateobs	Planck dateobs
			20100225, 20100226, 20100409, 20100410, 20100411, 20100412, 20100413, 20100414
J1743-0350	PLCKERC030 G021.60+13.15	20100915	20090914, 20100317
J1751+0939	PLCKERC030 G034.92+17.63	20100915	20090913, 20090914, 20100321
J1800+3848	PLCKERC030 G065.15+26.02	20100915	20090907, 20100329, 20100330
J1800+7828	PLCKERC030 G110.05+29.07	20101020	20091011, 20091012, 20100218, 20100219
J1806+6949	PLCKERC030 G100.12+29.18	20100704, 20100709, 20101109, 20101127	20091022, 20091023, 20100129, 20100130, 20100131, 20100511, 20100512, 20100513, 20100514
J1824+5651	PLCKERC030 G085.72+26.08	20100915	20090827, 20090828, 20090829, 20100417, 20100418
J1829+4844	PLCKERC030 G077.20+23.49	20100915	20090910, 20090911, 20090912, 20100411, 20100412
J1849+6705	PLCKERC030 G097.46+25.04	20100723, 20100803, 20100915, 20101020, 20101109	20091012, 20091013, 20091014, 20100117, 20100118, 20100119, 20100513, 20100514
J1927+7358	PLCKERC030 G105.63+23.54	20101020	20090928, 20090929, 20090930, 20100202, 20100203
J1955+5131	PLCKERC030 G085.28+11.76	20101020, 20101127, 20101120	20091203, 20091204, 20091205, 20100506, 20100507
J2005+7752	PLCKERC030 G110.45+22.73	20101020	20090925, 20090926, 20100209, 20100210
J2022+6136	PLCKERC030 G096.08+13.77	20100702, 20100723, 20100803	20100106, 20100107, 20100526, 20100527, 20100528
J2123+0535	PLCKERC030 G058.03-30.09	20101109, 20091115	20091110, 20091111, 20100509
J2134-0153	PLCKERC030 G052.38-36.49	20091115, 20091103	20091110, 20100509, 20100510
J2136+0041	PLCKERC030 G055.47-35.57	20101109, 20091115	20091112, 20100511
J2139+1423	PLCKERC030 G068.51-27.50	20101127, 20101120, 20091115	20091120, 20091121, 20100516
J2148+0657	PLCKERC030 G063.61-34.11	20091115	20091118, 20091119, 20100516
J2202+4216	PLCKERC030 G092.62-10.44	20091103	20091225, 20091226, 20100606, 20100607
J2203+1725	PLCKERC030 G075.68-29.62	20101127, 20101120, 20091103	20091201, 20091202, 20100524, 20100525
J2203+3145	PLCKERC030 G085.95-18.77	20100702, 20091103	20091214, 20091215, 20100531
J2218-0335	PLCKERC030 G059.05-46.63	20091115	20091121, 20091122, 20100522
J2225-0457	PLCKERC030 G058.96-48.81	20091115	20091123, 20100523, 20100524
J2229-0832	PLCKERC030 G055.15-51.70	20091115	20091122, 20100523, 20100524
J2232+1143	PLCKERC030 G077.45-38.54	20091103	20091206, 20100601
J2236+2828	PLCKERC030 G090.11-25.64	20100702, 20091103	20091220, 20091221
J2253+1608	PLCKERC030 G086.12-38.18	20100702, 20091103	20091215, 20091216
J2327+0940	PLCKERC030 G091.17-47.99	20100702, 20100723, 20100803	20091220, 20091221